


**Research Article**

## Articular Void Sign on MRI in Intra-Articular Distal Radius Fracture Patients

 Ryoichi Shibuya<sup>1,2</sup>

### Abstract

**Introduction:** MR imaging provides more information about tissue status than plain radiographs. The purposes of this study were to investigate the relationship between plain radiograph, MR imaging and wrist function in patients with intra-articular distal radius fracture treated using volar locking plate.

**Materials and methods:** The plain radiographs, CT scans, and MRI findings of 27 patients were examined. The mean follow-up was 2 years (1 year - 3 years and 6 months). The range of motion of the wrist joint was evaluated as % arc, which is the ratio of the range of motion to that on the healthy side, expressed as a percentage.

**Results:** In 27 patients, there were 6 type C1, 3 C2, and 18 C3 fractures. The mean step measured on plain radiographs was  $0.4 \pm 0.7$  mm (range, 0 to 2 mm), and that on T1-weighted MR image was  $0.6 \pm 0.9$  mm (range 0 to 3 mm). The mean % arc was  $88.1 \pm 11.3\%$  (range, 48.5 to 100 %). Plain radiographs showed an area of sclerotic change in the subchondral bone in three patients. In two of the three patients, the area corresponding to this sclerotic area was a homogenic low intensity area on the T1-weighted MR images. This area consists of components with unspecified shape and intensity on T2-weighted MR images and designated as “articular void”.

**Conclusions:** This articular void was considered to include necrotic bone, fibrous tissue and suggested to be one of a cause of impairment of joint function.

**Keywords:** Distal Radius Articular Fracture; Volar Locking Plate; MRI; Articular Void

### Introduction

Osteoarthritis of the articular surface [1] and fibrosis spreading into the joint [2] have been described as the main causes of functional impairment of the wrist joint after intra-articular distal radius fracture. An incongruity of the articular surface has been said to be the cause of osteoarthritis at the intra-articular distal radius fractures [1]. Nevertheless, there are many reports that one of the major causes of OA in knee joints is impaired subchondral bone circulation [3, 4, 5, 6]. As for the fibrosis in the wrist joint after intra-articular distal radius fracture, Gabl et al. detected arthrofibrosis spreading from the fracture line into the joint space using arthroscopic observations of wrist at the time of plate removal after bone fusion in 20 patients [2]. Arthrofibrosis in the knee and ankle joints was previously evaluated by magnetic resonance imaging (MRI) not only by the arthroscopy [7, 8]. While there are no reports of MRI evaluation of fibrosis for distal radius fractures,

### Affiliation:

<sup>1</sup>Department of Orthopedic Surgery, North Osaka Housenka Hospital

<sup>2</sup>Department of Orthopedic Surgery, Izumiotsu Municipal Hospital

### Corresponding author:

Ryoichi Shibuya. Department of Orthopedic Surgery, North Osaka Housenka Hospital 1-2-2 Muroyama, Ibaraki-shi, Osaka, 567-0052, Japan

**Citation:** Ryoichi Shibuya. Articular Void Sign on MRI in Intra-Articular Distal Radius Fracture Patients. *Journal of Radiology and Clinical Imaging* 6 (2023): 208-212.

**Received:** November 29, 2023

**Accepted:** December 08, 2023

**Published:** December 27, 2023

MRI provides a lot of information about the wrist joint, including suspected scaphoid fractures [9] and ischemic changes of the lunate [10]. However, the distal radius fracture after surgery with a volar locking plate (VLP) is difficult to visualize on MRI due to metal artifacts. Yamamoto et al. reported that the most common reason for the removal of hardware was routine removal [11]. VLPs were removed routinely after bone fusion at our institution as well. And these patients requested MRI. We hypothesized that 1) MRI could detect circulatory disturbances in the subchondral bone after intra-articular distal radius fractures, 2) MRI could show fibrosis in the wrist joint, and 3) these subchondral bone ischemia and fibrosis in joint might affect wrist function. The primary objective of this study is, In order to examine these hypotheses, to retrospectively investigate the MRI findings and wrist function of the patients with an intra-articular distal radius fractures treated with VLP after removal of hardware. In addition, since VLPs are still often not removed, a second objective is to examine the compatibility of plain radiographs and MRI findings.

## Patients and Methods

Between July 2010 and April 2014, 38 consecutive patients underwent open reduction and internal fixation (ORIF) for intra-articular DRF. ORIF using VLP (SmartLock, Stryker Germany) was performed. As three patients moved and one dead of stroke 6 months after surgery, four patients were lost of the follow up. Therefore, 34 patients were followed up for more than one year after surgery, and all had their hardware removed. Until April 2015 at our institution, hardware was removed as a routine procedure in all patients after bone fusion was obtained. Twenty-seven out of 34 patients requested MRI. In these 27 patients the plain radiographs, CT scans, MRI findings and wrist function of these patients were retrospectively evaluated with approval by the Ethics Committee of our institution. And informed consent was obtained from all patients. The mean postoperative follow-up of 27 patients was 2 years (range, between 1 year and 3 years and 6 months). At the time of surgery, the mean age of patients was 66.3 years (range, between 45 and 82 years). Before surgery, posteroanterior, lateral, and oblique radiographs of injured and uninjured wrists were acquired. and CT sections (BrightSpeed Elite, GE Yokokawa Medical System, Tokyo, Japan) of the wrist were acquired. AO/OTA classification was performed based on plain radiographs and CT images. Plain radiographs of the injured side were obtained immediately, 1, 3, 6, 9 months and 1 year after surgery, on the date of pre and post removal of the hardware and the last survey. MRI was performed after hardware removal. The mean time from surgery to MRI was 12 months (range, between 5 and 36 months), while that from plate removal to MRI was 7 weeks (range, between 1 and 37 weeks). Patients underwent MRI on the wrist using 1.5 T Philips Achieva (Philips Healthcare, the Netherlands). Conventional sequences including coronal, sagittal, and axial T1-weighted images (TR = 650 ms,

TE = 22 ms, field of view (FOV) = 12 x 12 cm, slice thickness = 3 mm), coronal T2-weighted images (TR = 3000 ms, TE = 90 ms, FOV = 12 x 12 cm, slice thickness = 3 mm) and coronal short tau inversion recovery (STIR) images (TR = 3000 ms, TE = 90 ms, TI = 140 ms, FOV = 12 x 12 cm, slice thickness = 3 mm) were used. On plain radiographs, gaps and steps on the surface were measured in the vertical and parallel directions relative to the axis of the radius respectively, as previously described by Kreder et al [12] in 0.5-mm increments (Fig. 1a). On MRI, the decreased intensity area, which was lower than the surrounding bone marrow in coronal T1-weighted images, was measured in 0.5-mm increments as a tentative gap (Fig. 1b). The step and gap in MRI were measured in coronal T1-weighted images as well as in plain radiographs to measure the step of the subchondral bone in 0.5-mm increments. The images of patients with characteristic features were investigated in detail and the results of physical examinations documented in medical records were examined. The range of motion of the wrist joint was evaluated as % arc, which is the ratio of the total value of palmar flexion and dorsiflexion to the value on the healthy side, expressed as a percentage.

## Statistical analysis

Power analysis was not performed due to the low number of patients in general. The relationship between two groups was assessed using a single regression analysis (StatView-J5.0, SAS, Cary, NC). All data are shown as means ± standard deviation and ranges. And ranges of 95 % confidence intervals were calculated and shown in graphs. P-values of <0.05 were considered to indicate significance.

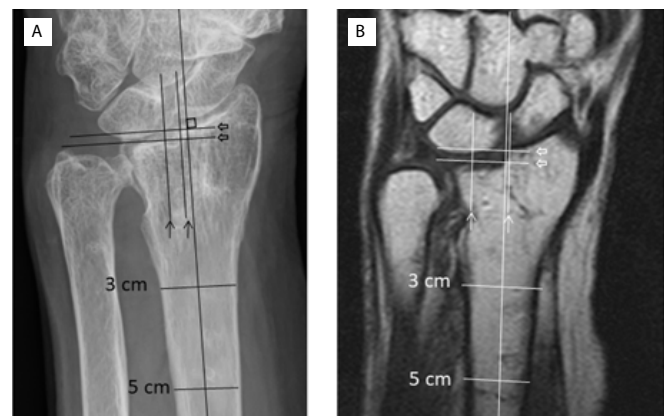


**Figure 1:** 78-year-old woman. Left: example of gap and step measurement of a plain radiograph obtained after 1 year and 7 months after surgery. The central axis was drawn according to Kreder's method from the midpoint 3 and 5 cm below the articular surface. Step was defined as the maximum level difference in the tidemark of the subchondral plate in the longitudinal direction relative to the axis of the radius, and gaps on the surface were measured quantitatively in the vertical direction relative to the axis of the radius. The gap was 3.0 mm (arrows), and the step was 2 mm (open arrows). Right: On a coronal T1-weighted image (right) 1 year and 4 months after surgery, the gap was 7.5 mm (arrows) and the step was 2.5 mm (open arrows).

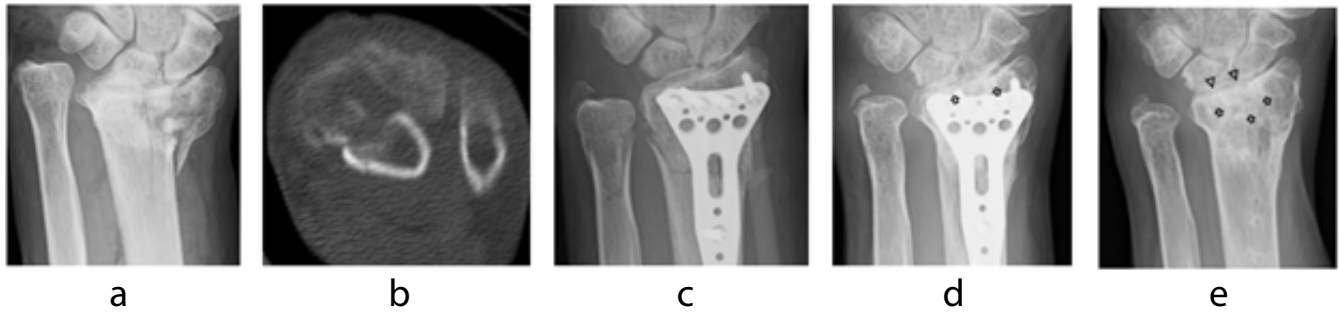


**Figure 2:** Patient 1, A 67-year-old female, housewife, anteroposterior and lateral views of plain radiographs

- (a) On preoperative plain radiograph, an AO type C3.2 intra-articular distal radius fracture. was observed.
- (b) Preoperative CT scan showed a central impaction fragment (Fig. 2b).
- (c) On plain radiograph immediately after surgery, no step or gap was present.
- (d) At 6 months postoperatively a plain radiograph showed a sclerotic image of the subchondral change through the plate (open arrows).
- (e) One year after surgery, there was no obvious step or gap; however, sclerosis of the subarticular bone was detected (open arrows) at the distal end of the radius and narrowing of the articular cleft (open arrow heads).

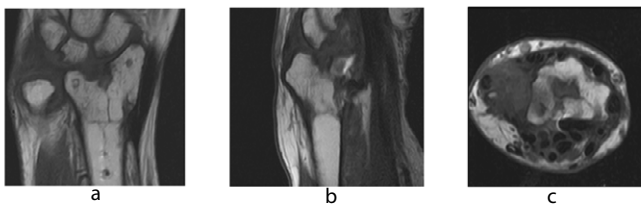


**Figure 3:** Patient 1. MRI 11 months after surgery

- (a) A coronal T1-weighted image showed a low signal intensity area (arrows) bordering the articular surface with a width of 9 mm.
- (b) Sagittal T1-weighted image demonstrated a low signal intensity area.
- (c) Axial T1-weighted images also represented a low signal intensity area (arrows) which was surrounded by a region of iso-intensity in the center of the articular surface.

## Results

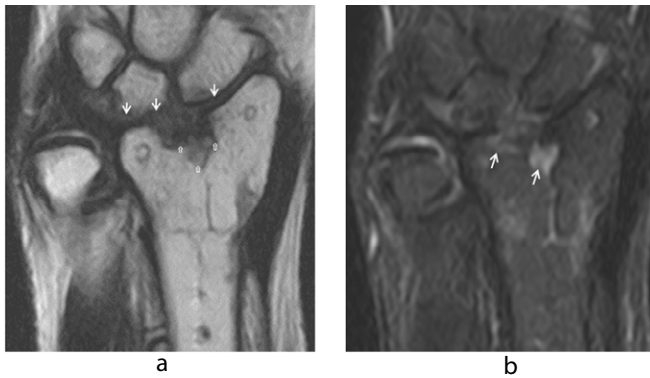
According to the AO/OTA classification, there were 6 type C1, 3 C2, and 18 C3 fractures. Comminuted central impaction fragments were observed in 9 patients on CT sections. The mean % arc was  $88.1 \pm 11.3\%$  (range, 48.5 % to 100 % degrees). There were three patients whose % arc was smaller than the standard deviation. Plain radiographs showed sclerotic change of the subchondral bone in three patients. These three patients were consistent with those three patients who had smaller % arc. Those values of them were 66.7 %, 68.8 % and 48.5 %. In current report they were designated as patient-1, patient-2 and patient-3, respectively. There were 5 patients with the largest 3 mm gap, and their % arcs were 82.4%, 85.3%, 68.8%, 93.5%, and 93.6%, respectively. Of these, only patient 2, with a % arc of 68.8%, was included in the three patients whose % arc was smaller than the standard deviation mentioned above. The mean gap measured on T1-weighted MR image was  $1.9 \pm 3.4$  mm (range 0 to 15 mm). The % arc of patient 1 with 9 mm gap on T1-weighted MR

image without joint surface irregularity on plain radiograph and patient 2 with 15 mm gap on T1-weighted MR image with 1 mm step and 3 mm gap were 68.8 % and 66.7 %, respectively. The area measured as a gap in T1-weighted MR images was a homogeneous low density area in T1-weighted MR images, while it was a heterogeneous intensity area in T2-weighted MR images, containing cord-like tissue from the subchondral bone into the joint. The mean step measured on plain radiographs was  $0.4 \pm 0.7$  mm (range, 0 to 2 mm), and that on T1-weighted MR image was  $0.6 \pm 0.9$  mm (range 0 to 3 mm). Only one patient showed a 2 mm step on plain radiograph with a % arc of 93.5%. The largest step among the 27 patients was 3 mm on coronal T1-weighted MR image in one patient. This patient was patient 3 of the above 3 patients whose % arc was less than the standard deviation.

## Clinical case

### Patient-1

A 67-year-old female. While walking, the patient fell. A plain radiograph (Fig. 2a) and CT scan showed AO type C3.2 and central impaction fragment (Fig. 2b). One week later, ORIF was performed using VLP and no gap and step were demonstrated on a plain radiograph at immediately after surgery (Fig. 2c). A plain radiograph at 6 months postoperatively showed no obvious gap or step, but a sclerotic change in the subchondral bone (Figs. 2d). The plate and screws were removed 9 months after surgery. MRI was performed 11 months after surgery. A coronal T1-weight image showed a low intensity area at the subchondral bone area with a width of 9 mm (Fig. 3a). On a sagittal T1-weighted image, a low intensity area was detected at the subchondral area (Fig. 3b). The axial T1-weighted image showed a hypointense area in the center of the articular surface (Fig. 3c). The T2-weighted image showed that this area was heterogeneous and contained iso-intensity tissue of irregular shape spanning from the



**Figure 4:** Patient 1. MRI 11 months after surgery.

(a) A coronal T2-weighted image showed a heterogeneous low and iso signal intensity area (open arrows). An iso-intensity cord-like tissue ran from the subchondral bone area to the joint space around the lunate scaphoid (closed arrows).

(b) A coronal STIR image demonstrated a high intensity small area in the subchondral bone.

subchondral bone to the scaphoid and lunate periphery (Fig. 4a). STIR imaging showed a high intensity small area in the subchondral bone (Fig. 4b). One year after surgery (1 month after MRI), a plain radiograph revealed sclerotic change of the subchondral bone and joint space narrowing without no gap or step (Fig. 2e). The osteosclerotic area on plain radiographs and the low intensity area on MR images were in the same location (Figs. 2e, 3a). A % arc of 66.7%. 3 years 6 months after surgery, plain radiograph showed subchondral bone sclerosis and joint space narrowing one year as with that at one year postoperatively.

## Discussion

In this study, there were three out of 27 patients whose % arc was lower than the mean subtracted standard deviation value. And three patients were found to have subchondral bone sclerosis on plain radiographs, all of whom were the same patient. Therefore, these three patients were designated as Patient-1, Patient-2, and Patient-3. Of these, the MRI feature common to both patient-1 and patient-2 was a homogeneously low intensity area on T1-weighted images (Figs. 3 and 7). And these homogeneously low intensity areas on T1-weighted images contained a gap at joint surface and its contiguous subchondral bone area that coincided to a sclerosis area on plain radiographs. Nevertheless, this area was heterogeneous on T2-weighted images, and was a combination of various intensities and shape components. We tentatively called it “articular void” because this area may not consist of certain components.

The subchondral region has abundant arterial and venous vessels that branch into the calcified cartilage of the adjacent articular cartilage [13]. Saini and Saifuddin mentioned that the most common trigger of osteonecrosis is trauma [14]. As for features on the image, in the early

stages of Kienböck syndrome, ischemia causes bone marrow edema and bone marrow intensity is low on T1-weighted images and high on T2-weighted images [15]. Complete bone marrow necrosis results in loss of signal intensity in both T1-weighted and T2-weighted images [16]. Saini and Saifuddin reported that advanced cases of osteonecrosis showed combinations of two or more tissue characteristics, such as bone sclerosis and fibrosis, within the same region [14]. For example, osteonecrosis of the femoral head, Vande Berg et al also detected focal regions that were homogeneous or heterogeneous, wedge-shaped, ovoid, bands, lines, rings, or crescents as other patterns [16]. The images of the articular void sign of the current patient-1 and patient-2 are very similar to the above (Figs. 3, 4), it was thought that at least the articular void sign on MRI included bone ischemic necrosis. And sclerotic bone on the plain radiograph suggested a probability of bone ischemic necrosis. On the other hand, Gabl et al. performed an arthroscopic examination at the time of plate removal on 20 patients after intra-articular DRF and found that fibrous tissue had expanded from the gap to the interosseous ligament and/or capsule [2]. Nevertheless, we did not find any MRI report of articular fibrosis after intra-articular distal radius fracture, Linklater and Fessa identified an intermediate signal on proton-density MRI due to edema and granulation in the early stages (approximately 6 months after surgery) in the ankle joint, whereas tissue was more organized with a lower intensity in long-term cases [17]. In current two patients, T2-weighted images, tissue with a iso or slightly high intensity signal, appeared to be continuous in a cord-like pattern from subchondral area to the carpal bone (Figs. 4, 8). This cord-like tissue was considered to be arthrofibrosis because it was in the joint space in which no bony component was observed on plain radiographs. It was suggested that the articular void sign in current patient-1 and patient-2 includes ischemic bone necrosis and fibrosis tissue at least. Patient-3 had a 3 mm step that could not be detected by plain radiograph but was revealed by tomography with MRI. Plain radiograph showed a sclerotic change of the subchondral bone, but MR image did not show any abnormal intensity in this area. In Patient-3, it was suggested that OA changes occurred due to incongruity as reported by Knirk and Jupiter [1], rather than ischemic changes. Currently, in many centers, the hard ware is rarely removed after distal radius fracture surgery, and MR images are often not available. Nevertheless, even if the articular surface appears to have been repaired on simple x-ray, if the postoperative simple x-ray shows osteosclerosis of the subchondral bone and is accompanied by dysfunction of the wrist joint, it is necessary to keep in mind the possibility that the step remains in the tomographic plane and that the subchondral bone of the articular surface has circulatory disturbance. The common preoperative features of current two patients with articular void sign are the presence of a central impaction fragments on preoperative CT scans. In this study, among 27 patients with

intra-articular fractures of the distal radius, nine had central impaction fragments on preoperative CT, and two of these nine had articular void signs. Central impaction fragments are not connected to surrounding soft tissues such as ligaments or joint capsules, which may be unfavorable to blood circulation. There are two limitations in this report 1) the sample size was small. and 2) a histological examination was not performed. However, we do not believe that it is ethically permissible to harvest tissue from a patient's joint site.

## Conclusion

In the present study, we discussed the presence of articular void at the distal end of the radius that exhibited a different intensity from that of normal bone marrow on MRI. It may contain extensive osteonecrosis of the subchondral bone and fibrosis which indicate joint surface impairment.

## References

- Knirk JL, Jupiter JB. Intra-articular fractures of the distal end of the radius in young adults. *J Bone Joint Surg Am.* 68 (1986): 647-659.
- Gabl M, Arora R, Klauser AS, et al. Characteristics of secondary arthrofibrosis after intra-articular distal radius fracture. *Arch Orthop Trauma Surg.* 136 (2016): 1181-1188.
- Felson DT, McLaughlin S, Goggins J, et al. Bone marrow edema and its relation to progression of knee osteoarthritis. *Ann Intern Med* 2003;139 (2003): 330-336.
- Hunter DJ, Zhang Y, Niu J, et al. Increase in bone marrow lesions associated with cartilage loss: a longitudinal magnetic resonance imaging study of knee osteoarthritis. *Arthritis Rheum* 54 (2006): 1529-1535.
- Garnero P, Peterfy C, Zaim S, et al. Bone marrow abnormalities on magnetic resonance imaging are associated with type II collagen degradation in knee osteoarthritis: a three-month longitudinal study. *Arthritis Rheum* 52 (2005): 2822-2829.
- Findlay DM. Vascular pathology and osteoarthritis. *Rheumatology* 2007; 46 (2007): 1763-1768.
- Bradley DM, Bergman AG, Dillingham MF. MR imaging of cyclops lesions. *Am J Roentgenol.* 174 (2000):719-726.
- Linklater JM, Fessa CK. Imaging findings in arthrofibrosis of the ankle and foot. *Semin Musculoskelet Radiol.* 16 (2012): 185-191.
- Gaebler C, Kukla C, Breitenheher M, et al. Magnetic resonance imaging of occult scaphoid fractures. *J Trauma* 1996;41:73-6.
- Ogawa T, Nishiura Y, Hara Y, et al. Correlation of histopathology with magnetic resonance imaging in Kienböck disease. *J Hand Surg Am.* 37 (2012): 83-89.
- Yamamoto M, Fujihara Y, Fujihara N, Hirata H. A systematic review of volar locking plate removal after radius fracture. *Injury.* 48 (2017): 2650-2656.
- Kreder HJ, Hannel DP, McKee M, Jupiter J, McGillivray G, Swiontkowski MF. X-ray film measurement for healed distal radius fractures. *J Hand Surg Am* 21 (1996): 31-39.
- Clark JM. The structure of vascular channels in the subchondral plate. *J Anat* 171 (1990): 105-115.
- Saini A, Saifuddin A. MRI of osteonecrosis. *Clinical Radiology.* 59 (2004): 1079-1093.
- Reinus WR, Conway WF, Totty WG, et al. Carpal avascular necrosis: MR imaging. *Radiology* 160 (1986): 689- 693.
- Vande Berg BC, Malghem J, Lecouvet FE, et al. Magnetic resonance imaging and differential diagnosis of epiphyseal osteonecrosis. *Semin Musculoskelet Radiol.* 5 (2001):57-67.
- Linklater JM, Fessa CK. Imaging findings in arthrofibrosis of the ankle and foot. *Semin Musculoskelet Radiol.* 16 (2012): 185-191.